miR-223 ameliorates thalamus hemorrhage-induced central poststroke pain via targeting NLRP3 in a mouse model

TIANFENG HUANG*, YINGGANG XIAO*, YANG ZHANG, CUNJIN WANG, XIAOPING CHEN, YONG LI, YALI GE and JU GAO

Department of Anesthesiology, Clinical Medical College of Yangzhou University, Northern Jiangsu People's Hospital, Yangzhou, Jiangsu 225001, P.R. China

Received March 6, 2021; Accepted January 28, 2022

DOI: 10.3892/etm.2022.11280

Abstract. Central poststroke pain (CPSP) is a central neuropathic pain syndrome that occurs following a stroke and mainly manifests as pain and paresthesia in the body region corresponding to the brain injury area. At present, due to the lack of clinical attention given to CPSP, patients suffer from long-term pain that seriously affects their quality of life. Current literature indicates that microRNA (miR)-223 can impede inflammation and prevent collateral damage. The NLR family pyrin domain containing 3 (NLRP3) inflammasome induces IL-18 and IL-1β secretion and maturation and participates in the inflammatory response. Previous evidence has confirmed that miR-223 can negatively regulate NLRP3 in the development of inflammatory responses. However, whether the miR-223 targeting of NLRP3 is involved in CPSP remains unclear. In the present study, the expression of miR-223 was detected by reverse transcription-quantitative PCR analysis. The expression levels of NLRP3, caspase-1, ASC, IL-18, IL-1β, ERK1/2, p-ERK1/2 and GFAP were detected by western blot analysis. The results demonstrated that thalamic hemorrhagic stroke triggered by microinjection of collagenase IV (Coll IV) into the ventral posterior lateral (VPL) nucleus results in pain hypersensitivity. miR-223 expression level were significantly reduced in the CPSP model. The expression levels of NLRP3, caspase-1, ASC, IL-18 and IL-1β were significantly increased in the CPSP model. The expression level of GFAP was detected to determine astrocyte activation. The results demonstrated that astrocyte activation induced by Coll IV produced a CPSP model. The p-ERK1/2 expression level was demonstrated to be significantly increased in the CPSP model. The introduction of an miR-223 agomir significantly attenuated thalamic pain and significantly decreased the levels of NLRP3, caspase-1, ASC and proinflammatory cytokines (IL-18 and IL-1β). Furthermore, introducing a miR-223 antagomir into the VPL nucleus of naïve mice mimicked thalamic pain and significantly increased the levels of NLRP3, caspase-1, ASC and proinflammatory cytokine levels (IL-18 and IL-1β). These results indicated that miR-223 inhibited NLRP3 inflammasome activity (caspase-1, NLRP3 and ASC), which ameliorated thalamus hemorrhage-induced CPSP in mice via NLRP3 downregulation. In conclusion, these results may determine the mechanisms underlying CPSP and facilitate development of targeted therapy for CPSP.

Correspondence to: Dr Ju Gao, Department of Anesthesiology, Clinical Medical College of Yangzhou University, Northern Jiangsu People's Hospital, 98 Nan Tong Western Road, Yangzhou, Jiangsu 225001, P.R. China
E-mail: gaoju_003@163.com

*Contributed equally

Key words: microRNA-223, NLR family pyrin domain containing 3, thalamic hemorrhage, central poststroke pain, mouse model

Introduction

Stroke is among the most important diseases that endanger human life and health in the world today, which affects 15 million people per year in the world, causing 5 million deaths and 5 million cases of disability (1). Stroke is the number one cause of death in China, with an increasing incidence of 8.7%/year and direct economic losses of more than CN¥100 billion annually (2-4). Central poststroke pain (CPSP) occurs after ischemic or hemorrhagic stroke and is lesion-related, with continuous or intermittent pain accompanied by paresthesia. CPSP is one of the central neuropathic pain syndromes and one of the severe sequelae of stroke (5). While epidemiologic reports have revealed that hemorrhagic strokes represent only 8-18% of all strokes, they contribute to higher mortality rates than ischemic stroke (6). Approximately 8-14% of patients who have experiences a stroke suffer from CPSP, particularly after hemorrhagic stroke (7). At present, there is a significant lack of understanding of the pathogenesis of CPSP (8). Understanding the underlying mechanism of hemorrhagic-induced thalamic pain could offer new approaches for managing this disorder.

The inflammasome is a complex composed of multiple proteins, mainly consisting of caspase-1, apoptosis-associated speck-like protein containing a CARD (ASC) and NOD-like receptor (NLR). The inflammasome regulates the body's innate immune system and senses microorganisms, metabolites and stress responses (9). At present, the NLR family pyrin domain containing 3 (NLRP3) inflammasome, which is present in the

cytoplasm and can detect and recognize intracellular microbial infection or sterile inflammation caused by other molecules, is the most thoroughly studied inflammasome (10). A large number of endogenous and exogenous substances can cause NLRP3 inflammasome oligomerization and caspase-1 activation, which therefore stimulates the secretion and maturation of IL-18 and IL-1β that participate in the regulation of the body's inflammatory response (11). Over the past few years, the association between the inflammasome and pain related to the production of proinflammatory cytokines has received increasing attention from the medical community. Previous studies have suggested that inflammasome dysfunction is closely related to complex regional pain syndromes (12), inflammatory headaches (13), gouty arthritis (14), lumbar disc herniation (15) and spinal cord pain (16).

MicroRNAs (miRNAs/miRs) are endogenous small noncoding RNAs with a size of ~22 nucleotides. miRNAs serve important roles in essential biological activities, including cell proliferation, differentiation and apoptosis, and can be paired with the 3'untranslated region (UTR) of mRNA target genes to negatively regulate the transcription process (17). Cumulative evidence suggests that the expression of a considerable number of miRNAs in the nervous system is differentially regulated during the development of neuropathic pain (18,19).

miR-223 is most highly expressed in bone marrow cells and negatively expressed in several illnesses, including inflammation, lymphoma, leukemia, influenza and hepatitis B (20). Previously, studies have reported that miR-223 can impede inflammation to prevent collateral impairment (21,22). Moreover, NLRP3 mRNA is a confirmed target of miR-223 (23). One study demonstrated that miR-223 can negatively target NLRP3, which stimulates the production of specific macrophages, and miR-223 is currently considered a regulatory molecule that participates in the development of inflammatory responses (24). However, none of the aforementioned previous studies have discussed whether miR-223 targeting of NLRP3 is involved in CPSP.

In the present study, the function of miR-223 in thalamic hemorrhage-induced CPSP processing in the central nervous system (CNS) was investigated. Furthermore, to provide innovative insight into the molecular mechanisms of CPSP, whether miR-223 directly interacts with and regulates NLRP3 inflammasome expression was further explored.

Materials and methods

Animals. The research protocol and animal experiments were approved by the Animal Care and Use Committee of the Medical College of Yangzhou University (Yangzhou, China; approval no. SYXK2017-0044) and conformed to the standards for animal use and care formulated by the Government of China (25). All experiments were carried out according to the protocol of the International Association for Pain Research (26). A total of 148 CD1 male mice (age, ~7-8 weeks,weight, ~25-30 g) were purchased from the Comparative Medical Center of Yangzhou University. All the mice were held in captivity in animal facilities and were maintained under a basic cycle of 12-h light/dark cycles, temperature (23±1˚C) and humidity (50±5%) with free access to food and water. Appropriate efforts were made to minimize suffering and only a small number of animals were used. To reduce variability within and between individuals in the measurement of behavior outcomes, the mice were trained to perform the behavioral test for 1-2 days before the experiment. For the behavioral tests, the experimenter did not know the treatment conditions. After the experiment, the animals were euthanized. Euthanasia was performed by cervical dislocation.

Hemorrhage-induced thalamic pain model. Isoflurane (5% induction; 2% maintenance) was administered to anesthetize the mice, which were then laid in a stereotactic frame. Collagenase IV (Coll IV; 0.01 U/10 nl, dissolved in saline solution; Sigma-Aldrich; Merck KGaA) was injected into the right ventral posterior medial (VPM) and ventral posterior lateral (VPL) nuclei of the thalamus (3.01-4.25 mm on the ventral side of the skull surface, posterior 1.30-1.95 mm on the lateral side of the midline and anterior-posterior to bregma 0.82-2.30 mm) under the guidance of stereotactic orientation (27) using a glass micropipette. The sham operation cohort was injected with 10 nl sterile physiological saline. Following administration, the glass micropipette was held in position for 10 min to enable the Coll IV to fully disperse and then the glass micropipette was gradually removed. Following microinjection, iodophor and sterile saline were used to perfuse the surgical area, which was later stitched with a wound clip.

NLRP3-small interfering (si)RNA microinjection. A total of 2 μl NLRP3-siRNA (160 μM; 5'-GTACTTAAATCGTGA AACA -3'; Guangzhou RiboBio Co., Ltd.) solution was diluted using 1 μl sterile 20% glucose solution (4X), mixed gently and spun down briefly. Subsequently, 1 μl of TurboFect *In vivo* Transfection Reagent (Thermo Fisher Scientific, Inc.) was added to the diluted NLRP3-siRNA solution and mixed immediately by pipetting. The sample was incubated for 15-20 min at room temperature and then incubated on ice. The mixed NLRP3-siRNA sample (500 nl; 20 μM) was microinjected into the VPM/VPL nuclei of the thalamus with a glass micropipette connected to a microsyringe pump, as aforementioned. Sequences for NLRP3-siRNA and the corresponding negative control are presented in Table I.

miR-223 agomir and antagomir microinjection. CY 09 (Bio-Techne), was used to determine whether thalamic pain mimicked by the miR-223 antagomir could be rescued and to offer a reference for the treatment of thalamic pain. CY 09 (10 mg/kg) or vehicle (equal volume of saline) was pre-administered via the tail vein 30 min before microinjection of miR-223 antagomir into the unilateral thalamus. Subsequently, CY 09 (10 mg/kg) or vehicle was administered via the tail vein every day until day 7. miR-223 agomir (5'-UGUCAGUUU GUCAAAUACCCCA-3') and its scrambled negative control (5'-UCGUUUUUACACGAUCACGGUUU-3'), and miR-223 antagomir (5'-UGGGGUAUUUGACAAACUGACA-3') and its scrambled negative control (5'-GAUCCUCGGUCCUAG UAGUUA-3') were synthesized by Shanghai GenePharma Co., Ltd. Prior to thalamus microinjection, the samples were mixed with Invivofectamine® 3.0 Reagent (Invitrogen; Thermo Fisher Scientific, Inc.). The mixed miR-223 agomir, antagomir or control samples (500 nl; 20 μM) were introduced into the thalamus using a glass micropipette linked to a microsyringe

Table I. Sequences for NLRP3-siRNA and the corresponding negative control.

Gene	Sequence (5'-3')
NLRP3-siRNA	F: CCUGGAAGACAUAGACUUUTT R: AAAGUCUAUGUCUUCCAGGTT
Negative control-siRNA	F: UUCUCCGAACGUGUCACGUTT R: ACGUGACACGUUCGGAGAATT

NLRP3, NLR family pyrin domain containing 3; siRNA, small interfering RNA; F, forward; R, reverse.

Table II. Sequence of primers (mouse) used for reverse transcription-quantitative PCR.

Gene	Sequence (5'-3')
U6	F: GCTTCGGCAGCACATATACTAAAAT R: CGCTTCACGAATTTGCGTGTCAT
miR-223	F: CGCTCCGTGTATTTGACAAGC R: AGCCACACTTGGGGTATTTGA

miR, microRNA; F, forward; R, reverse.

pump. The micropipette was detached 10 min after administration. The surgical area was washed using sterile saline and the cut was stitched.

Behavioral tests. Pain behavior tests, including cold, thermal and mechanical tests, were performed. First, the claw withdrawal frequency in response to mechanical stimulation was assessed as previously described (28). In brief, the mice were kept alone in a plexiglass compartment on a raised screen and allowed to adapt for 30 min. Two-adjusted von Frey filaments (calibrated at 0.07 and 0.4 g; Stoelting Co.) were utilized to rouse the hind paw for ~1-2 sec and this was repetitively performed 10 times at an interval of 5 min between the two hind paws. Quick withdrawal of the claws was regarded as a positive response. The withdrawal response of the claw for each of the 10 stimuli was quantified as a percentage of response frequency: (Sum of claw withdrawal times/10 trials) x100% = response frequency.

Subsequently, an Analgesia Meter (model, 336; IITC Life Science Inc.) was used to assess claw retraction latency to heat as previously described (28-31). In brief, mice were kept in a Plexiglas compartment on a glass plate. The beam radiated from the lightbox and spread to the midpoint of the sole surface of each of the hind paws. Rapid lifting of the rear claw was considered a gesture for turning off the light. The duration of illumination beam time was considered the claw latency time. In each case, five replicates were conducted with an interval of 5 min. A 20 sec stoppage time was utilized to prevent tissue damage.

Finally, the claw withdrawal latency for harmful cold (0˚C) was measured utilizing a cold aluminum plate as previously described (28-31). In brief, each mouse was kept in a Plexiglas compartment on a flat plate and the temperature was continuously monitored using a thermometer. The time interval between placement and the mouse jump sign was considered to be the claw jump delay. Because over time, mice gradually tolerate cold stimulation, each of the experiments was replicated in triplicate at 10-min intervals, as previously described (32). A 20 sec stoppage time was utilized to prevent tissue damage.

At 30 min post-completion of the pain behavior tests, the motor function test was performed, investigating placement, grip and righting reflex, as described previously (23). For placement reflexes, the hind legs were placed somewhat lower than the forelimbs, while the back of the hind paws touched the periphery of the bench. Then, whether the rear paw was reflexively positioned on the desktop was recorded. For grip reflex, the animal was laid on a wire grill and whether the hind claw grasped the line was noted. The animal was laid on his back on a horizontal plane for the righting reflex to record whether the mouse could instantly turn to the correct upright position. All the tests were replicated five times at 5-min intervals and the results were logged by computing the number of regular reflex actions/test.

Reverse transcription-quantitative PCR (RT-qPCR). For RT-qPCR, total RNA was extracted from the thalamus using TRIzol® reagent (Invitrogen; Thermo Fisher Scientific, Inc.) and RT was performed using ThermoScript Reverse Transcriptase (Thermo Fisher Scientific, Inc.). RT was performed in accordance with previously published reports (33,34). Amplification of the template (4 μl) was performed via qPCR. Each sample was run in triplicate in a 20 μ reaction with 250 nM forward and reverse primers, 10 μl SsoAdvanced Universal SYBR Green Supermix (Bio-Rad Laboratories), and 20 ng cDNA. PCR reactions were performed with an initial 3-min incubation at 95˚C, followed by 40 cycles at 95˚C for 10 sec, 60˚C for 30 sec, and 72˚C for 30 sec in a Bio-Rad CFX96 real-time PCR system. The primers are presented in Table II. U6 was employed as an internal control for normalization. Three samples of 20 μl each were analyzed. A 7500 Fast Real-Time PCR Detection System (Applied Biosystems; Thermo Fisher Scientific, Inc.) was used to perform qPCR. The $2^{-\Delta\Delta Cq}$ method was used to quantify expression levels (35).

Western blotting. Western blotting was performed as previously reported (33,34,36). Briefly, following protein concentration quantification by BCA assay, tissue from the thalamus were homogenized with ice-cold lysis buffer (10 mM Tris, 5 mM EGTA, 0.5% Triton X-100, 2 mM benzamidine, 0.1 mM phenylmethylsulfonyl fluoride, 40 μM leupeptin, 150 mM NaCl). The crude homogenate was centrifuged at 4˚C for 15 min at 1,000 g. The supernatants were collected for cytoplasmic protein detection. The pellets were further sonicated and dissolved in nucleus-soluble ice-cold buffer (1 M Tris-HCl, 1% SDS, and 0.1% Triton X-100). After the protein concentration was measured, total protein was heated for 5 min at 99˚C. Subsequently, SDS-PAGE using a 10% gel was performed to separate proteins, with 30 mg protein/well. Separated proteins were transferred to a PVDF membrane via wet transfer. The

membrane was blocked with 5% skimmed milk in TBS with 0.1% Tween-20 for 1 h. Subsequently, membranes were incubated overnight at 4˚C with the following primary antibodies: rabbit anti-caspase-1 (1:1,000; Cell Signaling Technology, Inc. cat. no. 24232), rabbit anti-ASC (1:1,000; Cell Signaling Technology, Inc.; cat. no. 67824), rabbit anti-NLRP3 (1:1,000; Cell Signaling Technology, Inc. cat. no. 15101), rabbit anti-IL-18 (1:1,000; Abcam; cat. no. ab243091), mouse anti-IL-1β (1:1,000; Cell Signaling Technology, Inc. cat. no. 63124), rabbit anti-phosphorylated (p)-ERK1/2 (1:2,000; Cell Signaling Technology, Inc. cat. no. 4370), rabbit anti-ERK1/2 (1:2,000; Cell Signaling Technology, Inc. cat. no. 4695), rabbit anti-GAPDH (1:5,000; Cell Signaling Technology, Inc. cat. no. 2118) and mouse anti-glial fibrillary acidic protein (GFAP; 1:2,000; Cell Signaling Technology, Inc. cat. no. 3670). Following the primary incubation membranes were incubated with goat HRP-conjugated anti-rabbit or anti-mouse antibody (1:3,000; Jackson ImmunoResearch Laboratories, Inc. cat. nos. 115-005-003, 111-005-003). TBS with 0.1% Tween-20 was used as washing reagent. The secondary antibody was incubated for 1-2 h at room temperature. Proteins were visualized using western peroxide reagent, Clarity Western ECL Substrate (Bio-Rad Laboratories, Inc.) and a ChemiDoc XRS system (Bio-Rad Laboratories, Inc.) with Image Lab 4.0 software (Bio-rad Laboratories, Inc.). Semi-quantification of band density was performed using ImageJ 1.8 software (National Institutes of Health).

Dual-luciferase reporter assay. The possible binding site between NLRP3 and miR-223 was identified using the online forecasting software TargetScan 7.2 (http://www.targetscan.org/mmu_72/). PC-12 cells were cultured with high-glucose DMEM (Gibco; Thermo Fisher Scientific, Inc.) containing 5% FBS (Gibco; Thermo Fisher Scientific, inc.) and 1% gentamicin (Gibco; Thermo Fisher Scientific, Inc.). Cells were incubated at 37˚C with 5% CO_2. PC-12 cells with a fusion rate of 60-70% were transfected with a luciferase reporter plasmid and miR-223 agomir or negative control (agomir scramble) (both Shanghai GenePharma Co., Ltd.). A plasmid vector encoding a mutant locus of NLRP3 (NLRP3 mut) for miR-223 binding and a plasmid vector encoding the wild-type locus of NLRP3 (NLRP3 wt) for miR-223 binding were designed and constructed. The NLRP3-3'-UTR primer sequences were synthesized by Shanghai GenePharma Co., Ltd. and are presented in Table III. Following sequence verification by Sanger sequencing, PC-12 cells were co-transfected with the NLRP3 mut plasmid (80 ng) or NLRP3 wt plasmid and the miR-223 agomir or negative control using Lipofectamine 2000® (Invitrogen; Thermo Fisher Scientific, Inc.) according to the manufacturer's protocol. Luciferase activity was quantified as the ratio of firefly to Renilla luciferase activity, which was evaluated using a Luciferase Assay System (Promega Corporation) following 48 h of transfection. The relative luciferase activity is presented as the ratio of the assessed luciferase activity to that of the *Renilla* control.

Statistical analysis. The mice were randomly allocated to different experimental cohorts. Data are presented as the mean ± SD. One-way ANOVA and two-way ANOVA were used to statistically compare the data. If the ANOVA results revealed significant differences, paired comparisons between the mean values were assessed using Tukey's post hoc test. All data were analyzed using SigmaPlot 12.5 (Systat Software, Inc.). $P<0.05$ was considered to indicate a statistically significant difference.

Table III. Sequences of primers for NLRP3-3'UTR for the dual-luciferase reporter assay.

Primer	Sequence (5'-3')
Forward	ACCTCAACAGTCGCTACACG
Reverse	TAGACTCCTTGGCGTCCTGA

NLRP3, NLR family pyrin domain containing 3.

Results

miR-223 expression levels decrease and NLRP3/ASC/caspase-1 protein expression levels increase following Coll IV-induced thalamic pain. Following the establishment of the hemorrhage-induced thalamic pain model, the results demonstrated that the hemorrhage was localized predominantly around the VPL and VPM of the thalamus, without extending into the internal capsule. No bleeding was observed in other brain regions following microinjection of Coll IV at the dose and volume used. As expected, microinjection of saline into the thalamus did not result in significant bleeding and a normal thalamic structure was exhibited.

Thalamus hemorrhage mice displayed intense and persistent abnormal mechanical pain, hyperalgesia and abnormal cold contralateral pain. The claw retraction frequency using 0.07 g and 0.4 g von Frey filaments (Fig. 1A and B) increased significantly compared with the saline control. Moreover, the claw retraction latency for heat (Fig. 1C) and cold (Fig. 1D) stimulation decreased significantly on the contralateral side following Coll IV microinjection into the thalamus compared with the saline control. These pain reactions occurred 1 day following microinjection and lasted for a minimum of 14 days following Coll IV microinjection. Saline microinjection had no effect on the frequency or latency of contralateral base claw contraction. Furthermore, neither Coll IV nor saline microinjection changed the frequency or latency of ipsilateral claw retraction (Fig. 1E-G).

Subsequently, whether miR-223 and NLRP3 inflammasome proteins were altered in the thalamus following hemorrhage-induced thalamic pain was investigated. In mice, hemorrhage-induced thalamic pain time-dependently induced a significant reduction in miR-223 expression levels (Fig. 1H) and a significant increase in NLRP3/ASC/caspase-1 protein expression levels (Fig. 1I-L) in the thalamus on the ipsilateral side of mice that received Coll IV compared with the saline group. Therefore, miR-223 expression levels decrease and NLRP3/ASC/caspase-1 protein expression levels increase following Coll IV-induced thalamic pain.

NLRP3-siRNA microinjection attenuates Coll IV-induced thalamic pain. Subsequently, whether NLRP3-siRNA microinjection into the ipsilateral thalamus could attenuate thalamus hemorrhage-induced pain was investigated. siRNA

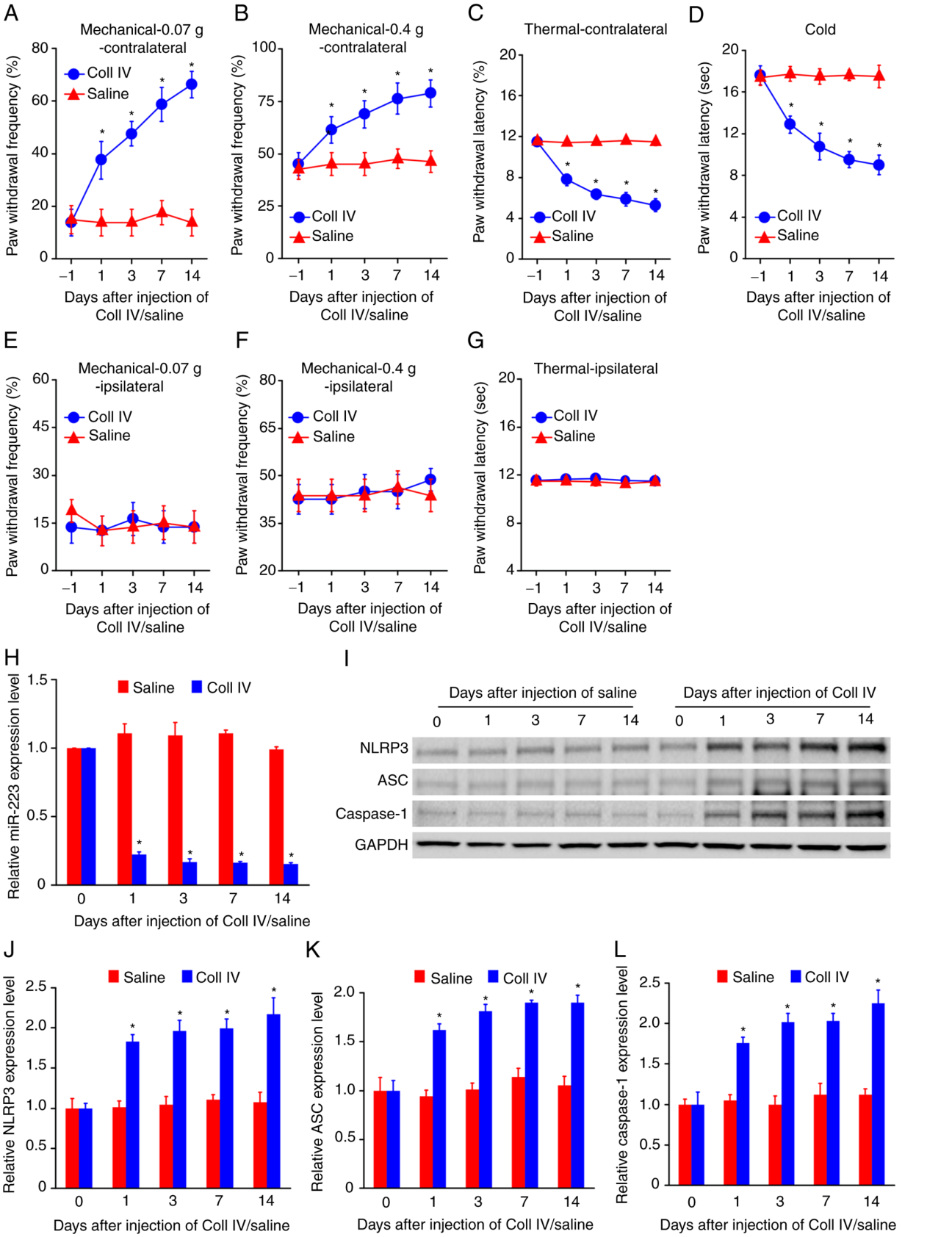

Figure 1. Hemorrhage-induced thalamic pain decreases miR-223 expression levels and activates the NLRP3 inflammasome. Microinjection of Coll IV, rather than saline, into the ventral posterior lateral and ventral posterior medial nuclei contributed to a significant increase in paw withdrawal frequency in response to (A) 0.07 g and (B) 0.4 g von Frey filaments and a significant decrease in paw withdrawal latency to (C) thermal and (D) cold stimuli on the contralateral side of the mice. (E-G) Both saline and Coll IV were injected into the ventral posterior lateral nuclei and ventral posterior medial nuclei, which did not change the ipsilateral side behavior. n=8 mice/group. (H) miR-223 expression levels were significantly reduced at day 1, 3, 7 and 14 days in the Coll IV-treated cohort. (I-L) The NLRP3 inflammasome was activated and caspase-1, ASC and NLRP3 were significantly elevated at day 1, 3, 7 and 14 in the Coll IV-treated group. n=3 mice/group. *P<0.05 vs. saline group at the corresponding time points. miR, microRNA; NLRP3, NLR family pyrin domain containing 3; Coll IV, collagenase IV; ASC, apoptosis-associated speck-like protein containing a CARD.

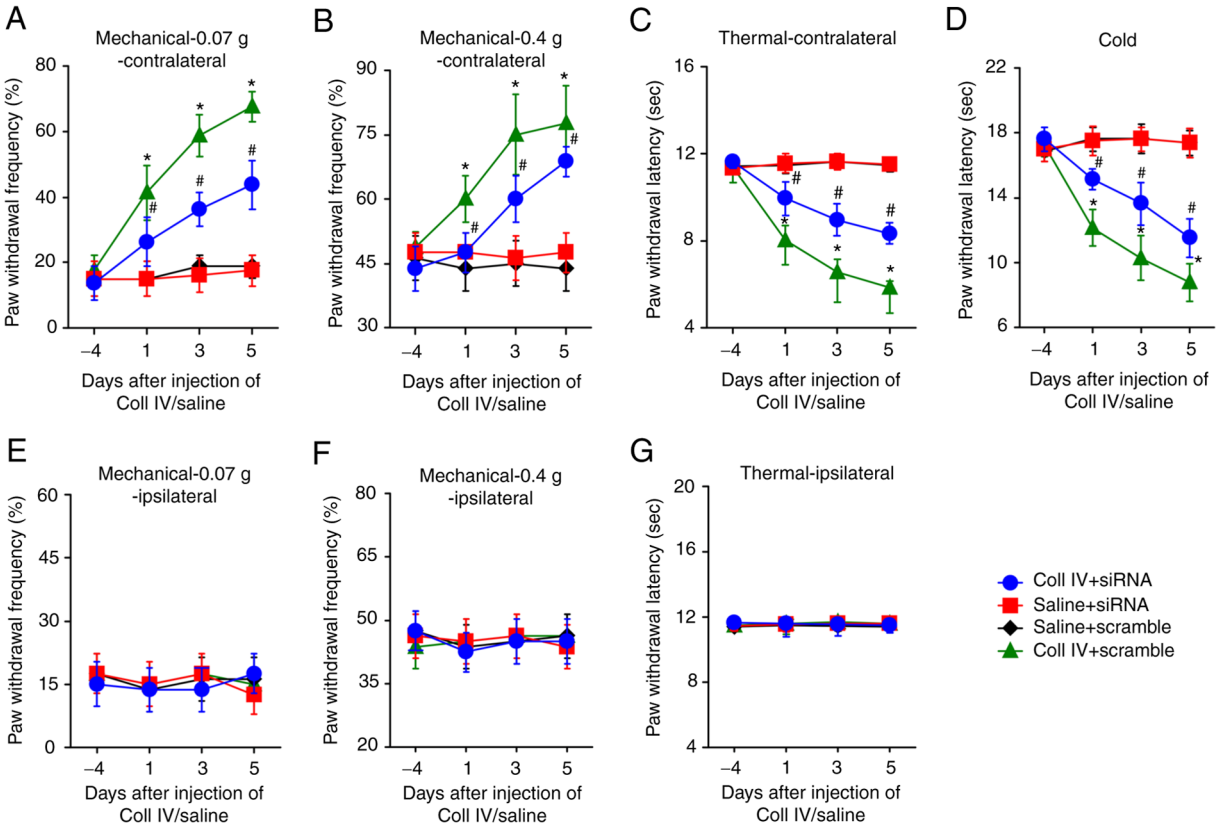

Figure 2. Effect of NLRP3-siRNA on thalamic pain. Baseline behavior tests were performed one day prior to siRNA/scramble injection into the VPL and VPM nuclei. Three days after the administration of siRNA or scramble, Coll IV or saline was microinjected into the VPL and VPM nuclei. Administration of siRNA significantly attenuated the increase in paw withdrawal frequency in response to (A) 0.07 g and (B) 0.4 g von Frey filaments and the decrease in paw withdrawal latency to (C) thermal and (D) cold stimuli at day 1, 3 and 5 following Coll IV microinjection on the contralateral side. (E-G) Administration of siRNA or scramble did not cause behavioral alterations on the ipsilateral side. n=8 mice/group. *P<0.05 vs. saline + scramble at the corresponding time points; $^{\#}$P<0.05 vs. Coll IV + scramble at the corresponding time points. NLRP3, NLR family pyrin domain containing 3; siRNA, small interfering RNA; VPL, ventral posterior lateral; VPM, ventral posterior medial; Coll IV, collagenase IV.

microinjection was performed 3 days prior to saline or Coll IV microinjection at the same coordinate points of the ipsilateral thalamus. The results demonstrated that thermal hyperalgesia, mechanical allodynia and cold allodynia significantly developed at day 1, 3 and 5 following Coll IV microinjection on the contralateral side of the thalamus in Coll IV + scramble group compared with the saline + siRNA group (Fig. 2A-D). Pretreatment with NLRP3-siRNA via microinjection significantly attenuated the increase in paw withdrawal frequency in response to 0.07 g and 0.4 g von Frey filaments and reduced the paw withdrawal latency to heat and cold at 1, 3 and 5 days following Coll IV microinjection on the contralateral side in the Coll IV + siRNA compared with the Coll IV + scramble group. Moreover, microinjection of NLRP3-siRNA had no effect on the basal PWF or PWL on the ipsilateral side in the Coll IV + siRNA group (Fig. 2E-G) or on both the contralateral and ipsilateral sides of the saline + siRNA group throughout the experiment. Therefore, NLRP3-siRNA microinjection attenuates Coll IV-induced thalamic pain.

NLRP3-siRNA microinjection decreases NLRP3 inflammasome activation. Following the behavioral tests, brain tissues were obtained for western blotting. The results demonstrated that NLRP3/ASC/caspase-1 protein expression levels in the ipsilateral thalamus were significantly elevated in the Coll IV + scramble group compared with the saline + scramble group (Fig. 3A). However, NLRP3/ASC/caspase-1 protein expression levels were significantly reduced in the Coll IV + siRNA group compared with the Coll IV + scramble group.

Furthermore, the protein expression levels of the inflammatory factors, IL-18 and IL-1β, in the ipsilateral thalamus were investigated. The results demonstrated that IL-18 and IL-1β protein expression levels were significantly elevated in the Coll IV + scramble group compared with the saline + scramble group (Fig. 3B). However, IL-1β and IL-18 protein expression levels were significantly reduced in the Coll IV + siRNA group compared with the Coll IV + scramble group.

The western blotting results also demonstrated that GFAP, a marker for astrocyte hyperactivation, and p-ERK1/2, a marker for central sensitization, were significantly elevated in the ipsilateral thalamus in the Coll IV + scramble group compared with the saline + scramble group (Fig. 3C). However, this was significantly reversed in the Coll IV + siRNA group compared with the Coll IV + scramble group. Therefore, NLRP3-siRNA microinjection decreases NLRP3 inflammasome activation.

miR-223 agomir microinjection attenuates Coll IV-induced thalamic pain. Subsequently, whether microinjection of miR-223 agomir into the ipsilateral thalamus could attenuate

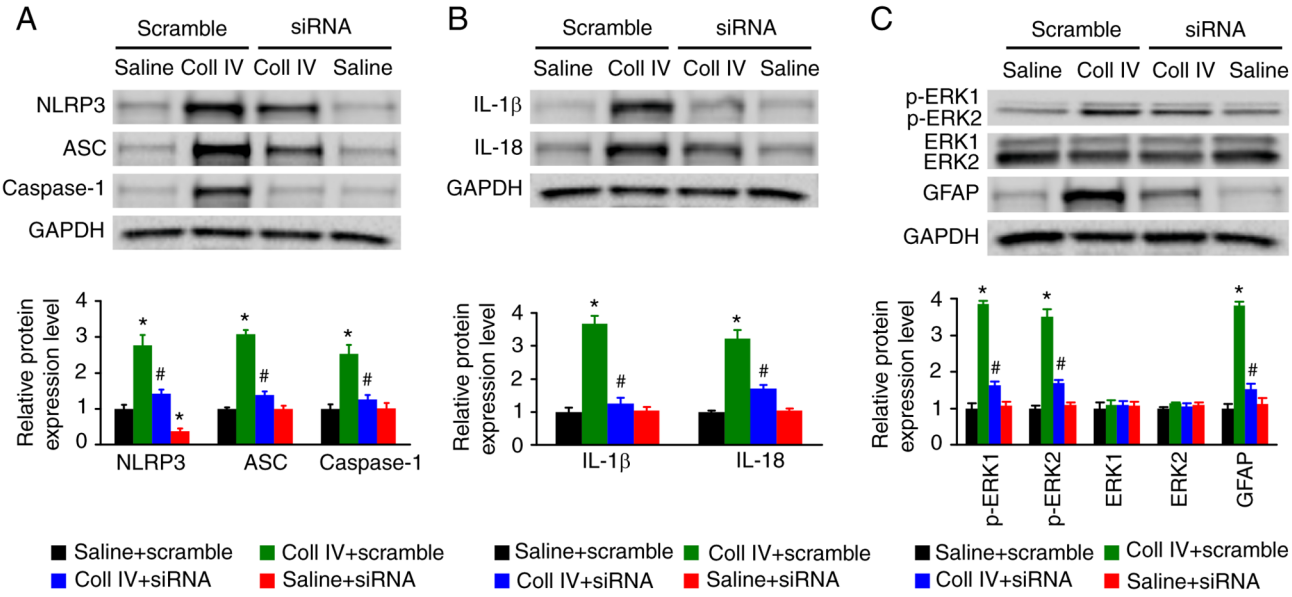

Figure 3. Effect of NLRP3 siRNA on NLRP3 inflammasome activity and the downstream factors IL-18, IL-1β, GFAP and p-ERK1/2. (A) Transfection with NLRP3 siRNA significantly decreased the protein expression levels of caspase-1, ASC and NLRP3. (B) NLRP3 siRNA also significantly reduced IL-18 and IL-1β protein expression levels. (C) After microinjection of NLRP3 siRNA, the protein expression levels of p-ERK1/2 and GFAP significantly decreased. n=3 mice/group. *P<0.05 vs. saline + scramble; #P<0.05 vs. Coll IV + scramble. NLRP3, NLR family pyrin domain containing 3; siRNA, small interfering RNA; GFAP, glial fibrillary acidic protein; p, phosphorylated; ASC, apoptosis-associated speck-like protein containing a CARD.

thalamus hemorrhage-induced pain was examined. miR-223 agomir microinjection was performed 3 days prior to saline or Coll IV microinjection at similar coordinate points of the ipsilateral thalamus. The results demonstrated that thermal hyperalgesia, mechanical allodynia and cold allodynia significantly developed at day 1, 3 and 5 following Coll IV microinjection on the contralateral side in the Coll IV + agomir scramble group compared with the saline + agomir-scramble group (Fig. 4A-D). Pre-administration of miR-223 agomir via microinjection significantly attenuated the increase in PWF in response to 0.07 g and 0.4 g von Frey filaments and the reduction in PWL to heat and cold stimuli at day 1, 3 and 5, in the Coll IV + miR-233 agomir group compared with the Coll IV + agomir-scramble group. Furthermore, microinjection of the miR-223 agomir had no effect on the basal PWF and PWL on the ipsilateral side in the Coll IV + miR-223 agomir group (Fig. 4E-G), or on both the contralateral and ipsilateral sides in the saline + miR-223 agomir group throughout the experiments. Therefore, miR-223 agomir microinjection attenuates Coll IV-induced thalamic pain.

miR-223 reduces NLRP3 inflammasome activation by binding to the NLRP3-3'-UTR. To examine the possible molecular mechanism involved in miR-223 regulation of thalamic pain, bioinformatic analysis was performed to identify direct target genes of miR-223. The results indicated that the NLRP3-3'-UTR contained a conserved miR-223 binding site and an RNA mutant sequence of the 3'-UTR of NLRP3 was indicated in the alignment (Fig. 5A). The interplay between the 3'-UTR of NLRP3 and miR-223 was confirmed by co-transfecting PC-12 cells with the NLRP3 wt plasmid or NLRP3 mut plasmid and miR-223 agomir or agomir scramble using Lipofectamine 2000 transfection reagent. The results from the dual-luciferase reporter assay indicated that miR-223 significantly reduced the luciferase activity of the wt 3'-UTR compared with the miR-233 group but had no effect on the mut 3'-UTR of NLRP3. These results therefore validated that NLRP3 may be a target gene of miR-223 (Fig. 5B).

Moreover, the results demonstrated that miR-223 expression levels were significantly lower in the agomir-scramble + Coll IV group compared with the agomir-scramble + saline group (Fig. 5C). Furthermore, miR-223 expression levels were significantly elevated in the ipsilateral thalamus in both the miR-223 agomir + Coll IV- or saline-treated cohort compared with the agomir-scramble + Coll IV and agomir-scramble + saline groups, respectively. Subsequently, the protein expression levels of activated caspase-1, ASC and NLRP3 in the thalamus of thalamic pain model mice, pretreated with miR-223 agomir or agomir scramble on the day 5 following surgery, were evaluated via western blotting. The results demonstrated that caspase-1, ASC and NLRP3 protein expression levels were significantly increased in the thalamus in the Coll IV + agomir-scramble group compared to the saline + agomir scramble group (Fig. 5D). Moreover, overexpression of miR-223 (Coll IV + agomir), compared with the Coll IV + agomir-scramble group, significantly reduced the caspase-1, ASC and NLRP3 protein expression levels in the thalamus. The IL-18 and IL-1β protein expression levels in the thalamus were also assessed using western blot analysis. The results demonstrated that the protein expression levels of both cytokines were significantly elevated in the Coll IV + agomir-scramble group compared with the saline + agomir-scramble group (Fig. 5E). However, IL-18 and IL-1β protein expression levels were significantly reduced in the Coll IV + agomir group compared to the Coll IV + agomir-scramble group. These results were further verified by the interplay between NLRP33 and miR-223, which illustrated that miR-223 may negatively regulate

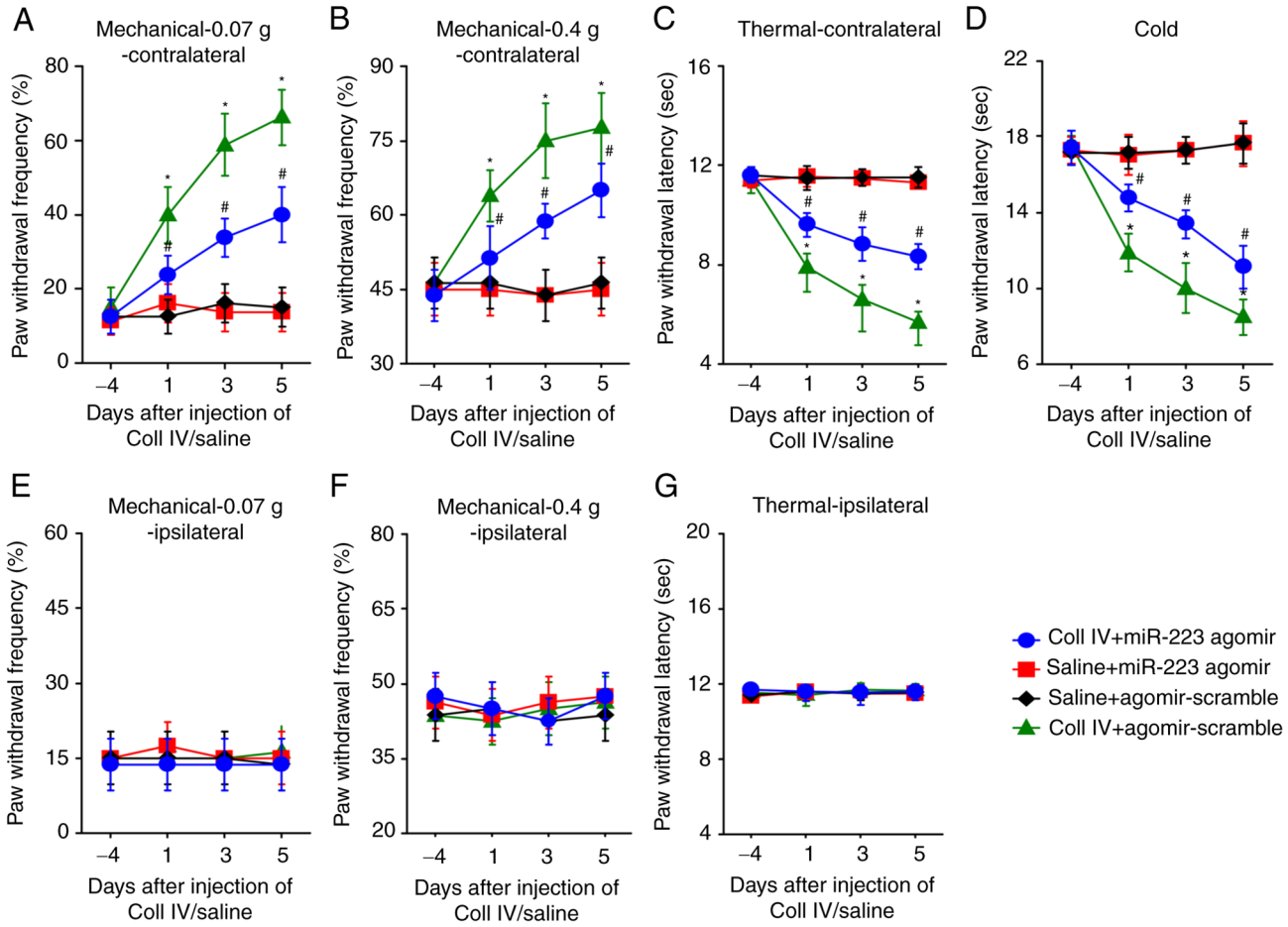

Figure 4. Effect of miR-223 agomir on thalamic pain. Baseline behavior tests were performed 1 day prior to miR-223 agomir or agomir-scramble microinjection into the VPL and VPM nuclei. Three days after administration of miR-223 agomir/agomir scramble, Coll IV or saline was microinjected into the VPL and VPM nuclei. Administration of miR-223 agomir significantly attenuated the increase in paw withdrawal frequency in response to (A) 0.07 g and (B) 0.4 g von Frey filaments and the significant decrease in paw withdrawal latency to (C) thermal and (D) cold stimuli on day 1, 3 and 5 following Coll IV microinjection on the contralateral side. (E-G) Administration of miR-223 agomir or agomir scramble did not affect behavioral changes on the ipsilateral side. n=8 mice/group. *P<0.05 vs. saline + agomir-scramble at the corresponding time points; $^{\#}$P<0.05 vs. Coll IV + agomir-scramble at the corresponding time points. miR, microRNA; VPL, ventral posterior lateral; VPM, ventral posterior medial; Coll IV, collagenase IV.

NLRP3 expression and thereby inhibit inflammatory activity (caspase-1, ASC and NLRP3) and cytokine maturation.

It was also demonstrated that GFAP and p-ERK1/2 protein expression levels were significantly higher in the Coll IV + agomir-scramble group compared with saline + agomir-scramble group (Fig. 5F). However, the high expression levels of GFAP and p-ERK1/2 were significantly reversed by miR-223 overexpression in the Coll IV + agomir group compared with the Coll IV + agomir-scramble group. These findings indicated that miR-223 may negatively regulate central sensitization and astrocyte hyperactivation. Therefore, miR-223 reduces NLRP3 inflammasome activation by binding to the NLRP3-3'-UTR.

miR-223 antagomir mimics thalamic pain and activates the NLRP3 inflammasome. It was then determined whether mimicking thalamic pain through a decrease in miR-223 via microinjection of the miR-223 antagomir into the unilateral thalamus altered the nociceptive thresholds in naïve mice. The results demonstrated that miR-223 expression levels in the microinjected thalamus from miR-223 antagomir-injected mice were significantly decreased compared with naïve + antagomir scramble group (Fig. 6H). Microinjection of miR-223 antagomir, but not scramble antagomir, produced significantly augmented paw withdrawal responses to cold, heat and mechanical stimuli on the contralateral side compared with the naïve group (Fig. 6A-D). On the ipsilateral side, the basal paw withdrawal responses did not changed in either the miR-223 antagomir-microinjected or scramble antagomir-microinjected mice (Fig. 6E-G).

The results also demonstrated that the NLRP3 inflammasome was activated, with significantly elevated NLRP3/ASC/caspase-1 protein expression levels in the miR-223 antagomir-microinjected compared with the naïve group, but not in the antagomir scramble-microinjected mice (Fig. 6I). Furthermore, the IL-18 and IL-1β protein expression levels were significantly increased in the miR-223 antagomir-microinjected mice compared with the scramble-microinjected mice (Fig. 6J). p-ERK1/2 and GFAP protein expression levels were also demonstrated to be significantly upregulated following miR-223 antagomir microinjection into the thalamus compared with the naïve group (Fig. 6K). Therefore, miR-223 antagomir mimics thalamic pain and activates the NLRP3 inflammasome.

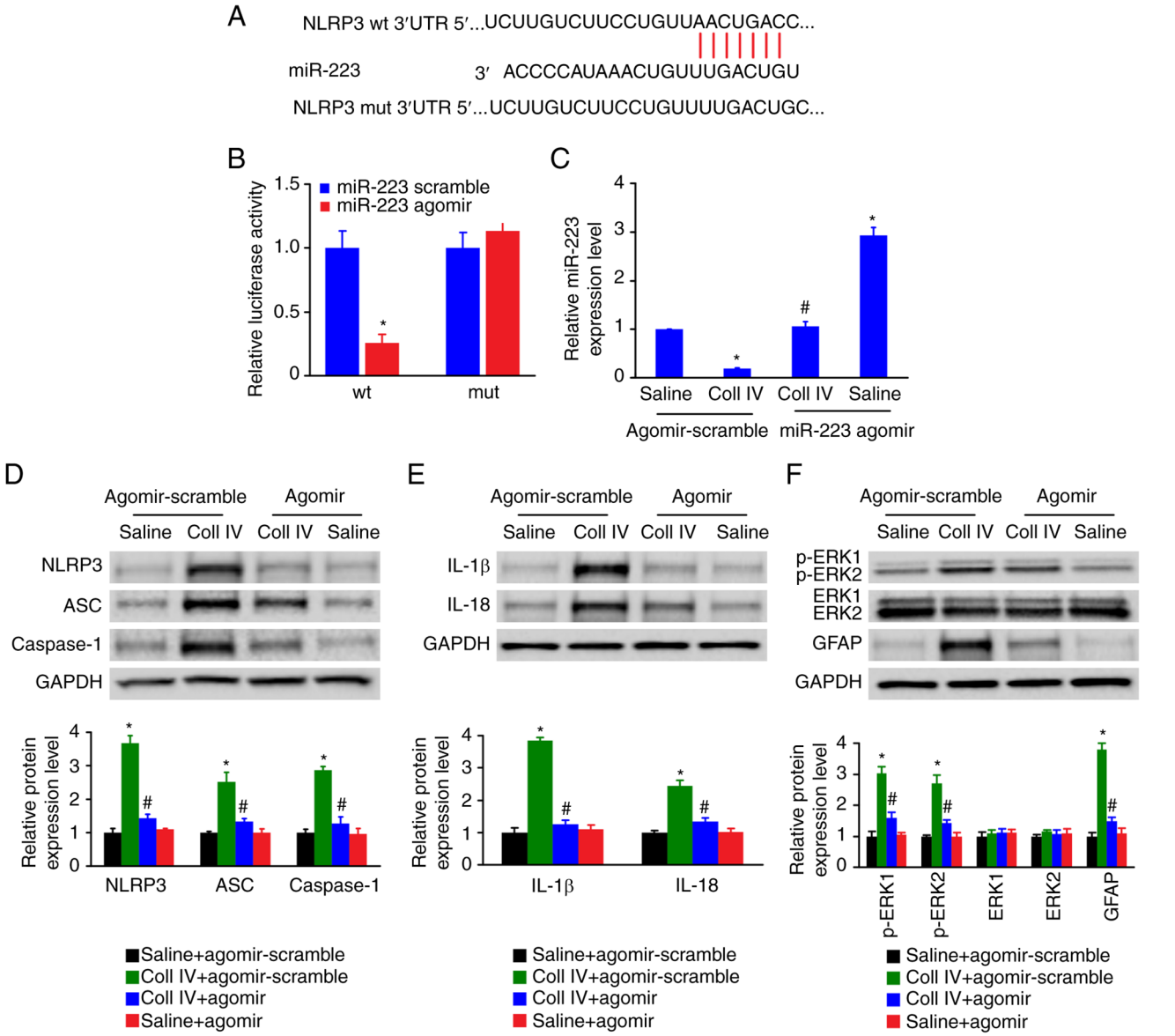

Figure 5. miR-223 targets the NLRP3 3'UTR and affects the protein expression levels of caspase-1, ASC, NLRP3, IL-18, IL-1β, p-ERK1/2 and GFAP. (A) Binding site of miR-223 within the NLRP3 3'-UTR. (B) miR-223 agomir significantly reduced the relative luciferase activity in PC12 cells transfected with the NLRP3 3'-UTR. (C) miR-223 agomir significantly increased miR-223 expression levels. (D) Administration of miR-223 agomir significantly reduced the protein expression levels of caspase-1, ASC and NLRP3. (E) miR-223 agomir also significantly reduced the expression of IL-18 and IL-1β. (F) After microinjection of miR-223 agomir, p-ERK1/2 and GFAP protein expression levels significantly decreased. n=3 mice/cohort. *P<0.05 vs. saline + agomir-scramble; #P<0.05 vs. Coll IV + agomir-scramble. miR, microRNA; NLRP3, NLR family pyrin domain containing 3; UTR, untranslated region; GFAP, glial fibrillary acidic protein; p, phosphorylated; ASC, apoptosis-associated speck-like protein containing a CARD; wt, wild-type; mut, mutant.

Mimicked thalamic pain induced by the miR-223 antagomir is rescued by an NLRP3 inflammasome inhibitor. In the present study it had been demonstrated that miR-223 targeted the NLRP3 3'-UTR and negatively regulated NLRP3. To determine whether a decrease in miR-223 expression levels produced thalamic pain by activating the NLRP3 inflammasome, a specific NLRP3 inflammasome inhibitor (37). Vehicle pretreatment 30 min before microinjection of miR-223 antagomir still yielded significantly increased paw withdrawal responses to cold, heat and mechanical stimuli on the contralateral side compared with the naïve group (Fig. 7A-D). However, this behavioral change was significantly reversed following CY 09 administration when compared with the naïve + miR-223 antagomir + vehicle group. These results suggested that CY 09 pretreatment 30 min before miR-223 antagomir microinjection significantly attenuated paw withdrawal responses to cold, heat and mechanical stimuli on the contralateral side. On the ipsilateral side, the basal paw withdrawal responses did not change in any cohort (Fig. 7E-G).

Subsequently, whether CY 09 could influence the IL-18, IL-1β, GFAP and p-ERK1/2 protein expression levels was investigated. The results first determined that miR-223 expression levels were significantly reduced in the miR-223 antagomir microinjection groups, compared with the naïve group, but not in the antagomir scramble microinjection cohorts. Moreover, CY 09 did not affect the expression of miR-223 (Fig. 8A). It was demonstrated that in the miR-223 antagomir mimic thalamic pain groups, IL-18 and IL-1β protein expression levels were

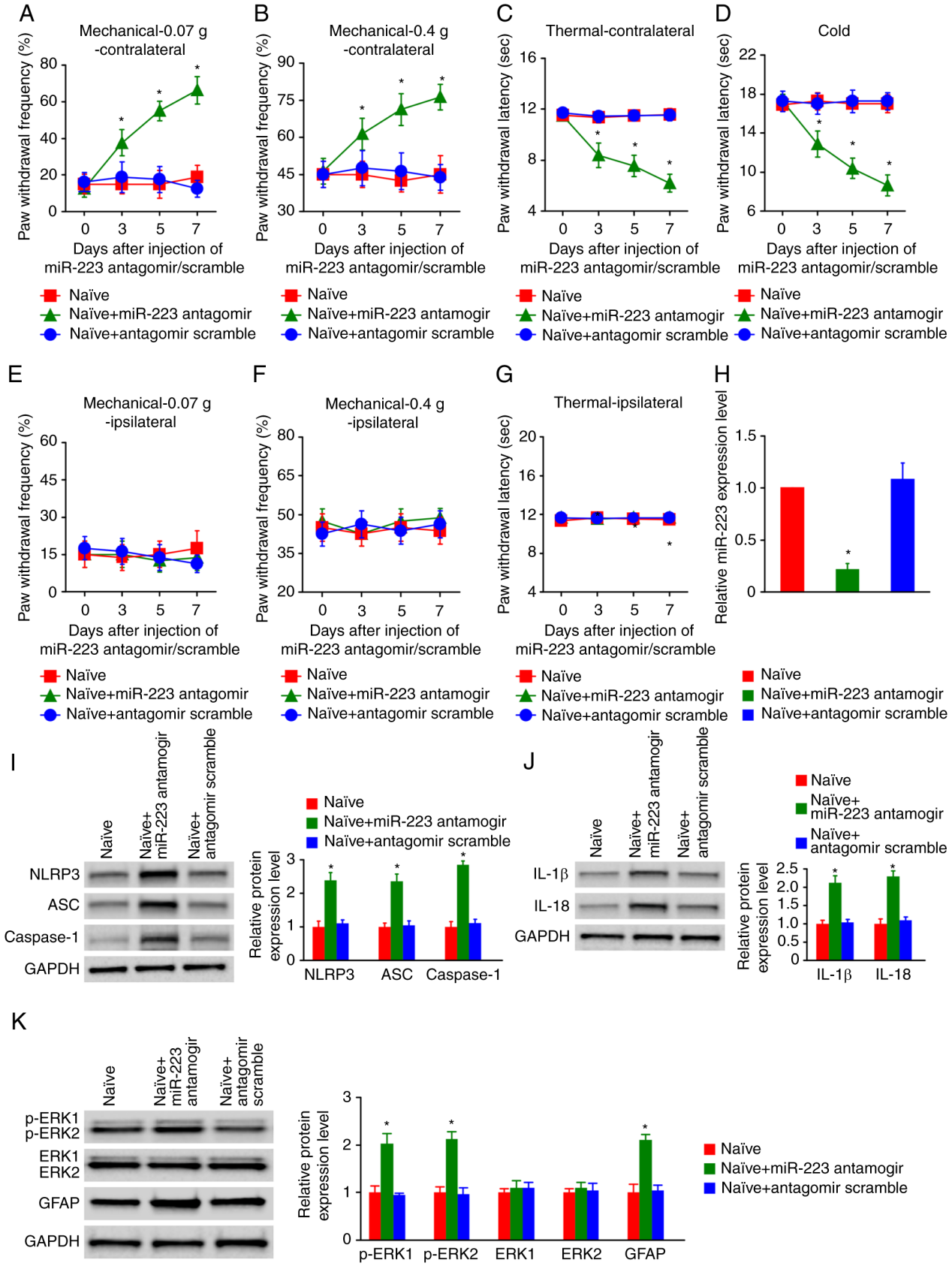

Figure 6. Effect of miR-223 antagomir on the nociceptive threshold in naïve mice. Administration of miR-223 antagomir contributed to a significant increase in the paw withdrawal frequency in response to (A) 0.07 g and (B) 0.4 g von Frey filaments and a significant decrease in paw withdrawal latency to (C) thermal and (D) cold stimuli on day 3, 5 and 7 on the contralateral side. (E-G) Administration of miR-223 antagomir or antagomir-scramble did not contribute to behavioral changes on the ipsilateral side. n=8 mice/group. (H) miR-223 antagomir significantly reduced miR-223 expression levels. (I) Administration of miR-223 antagomir significantly elevated caspase-1, ASC and NLRP3 protein expression levels. (J) miR-223 antagomir also significantly elevated IL-18 and IL-1β protein expression levels. (K) Following microinjection of miR-223 antagomir, p-ERK1/2 and GFAP protein expression levels increased. n=3 mice/group. *P<0.05 vs. naïve group. miR, microRNA; NLRP3, NLR family pyrin domain containing 3; GFAP, glial fibrillary acidic protein; p, phosphorylated; ASC, apoptosis-associated speck-like protein containing a CARD.

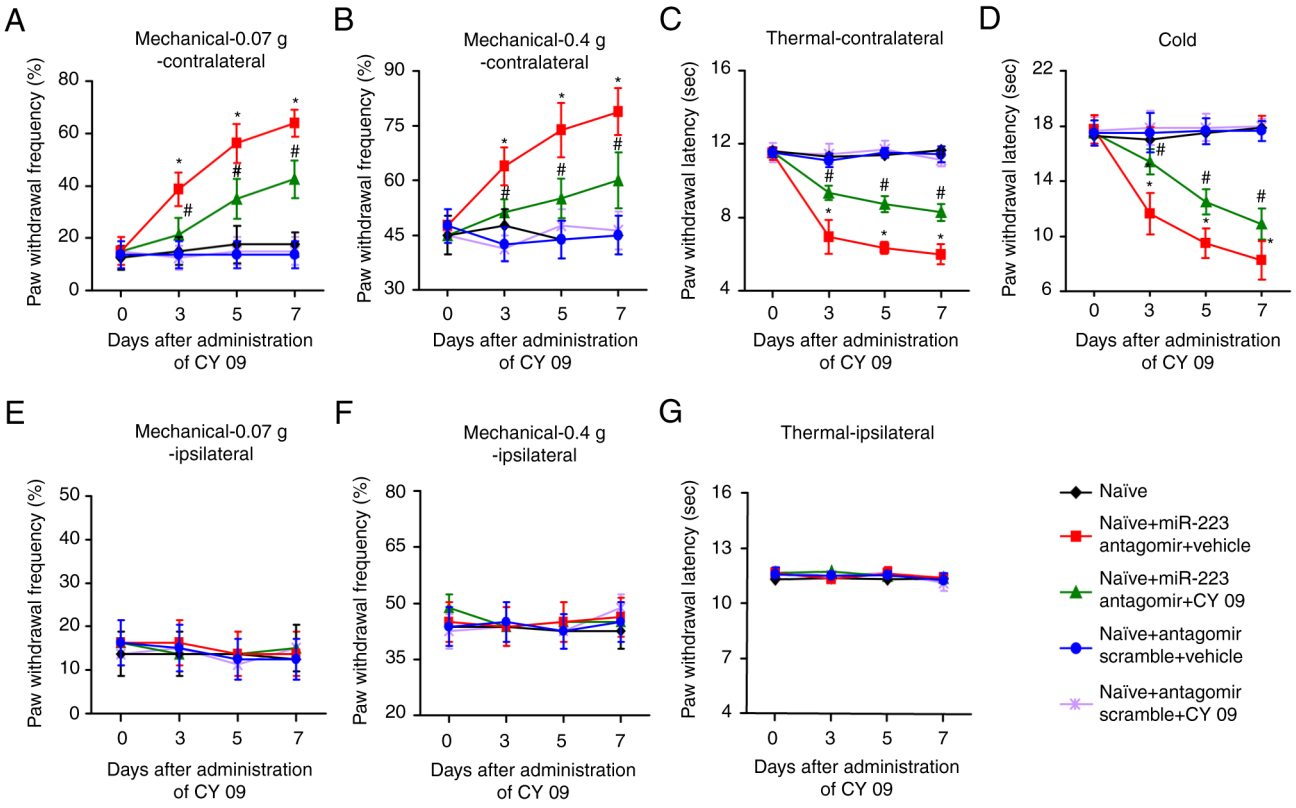

Figure 7. NLRP3 inflammasome inhibitor rescues miR-223 antagomir-induced thalamic pain in naïve mice. Tail vein injection of CY 09 (10 mg/kg) significantly attenuated the increase in paw withdrawal frequency in response to (A) 0.07 g and (B) 0.4 g von Frey filaments and the decrease in paw withdrawal latency to (C) thermal and (D) cold stimuli on day 3, 5 and 7 on the contralateral side. (E-G) Injection of CY 09 or vehicle did not cause behavioral changes on the ipsilateral side. n=8 mice/group. *P<0.05 vs. naïve group at the corresponding time points; #P<0.05 vs. naïve + miR-223 antagomir + vehicle group at the corresponding time points. NLRP3, NLR family pyrin domain containing 3; miR, microRNA.

significantly reduced with CY 09 pretreatment compared to vehicle + miR-233 antagomir group (Fig. 8B). These results suggested that CY 09 may specifically inhibit inflammasome activity and subsequently reduce IL-18 and IL-1β protein expression levels. Furthermore, it was determined that GFAP and p-ERK1/2 protein expression levels were also considerably reduced in the miR-223 antagomir + CY 09 pretreatment group compared with the miR-223 antagomir + vehicle pretreatment group (Fig. 8C). These findings indicated that activation of the NLRP3 inflammasome may contribute to central sensitization and astrocyte hyperactivation. Therefore, mimicked thalamic pain induced by the miR-223 antagomir is rescued by an NLRP3 inflammasome inhibitor.

Discussion

Thalamic hemorrhagic stroke is a common cerebrovascular event with severe consequences for CPSP patients (38). Evidence has confirmed that inflammation and the immune response participate in the pathophysiology of hemorrhagic stroke and activated glial cells accumulate at the site of bleeding injury (39). As a severe sequela of stroke, CPSP currently lacks effective treatments due to its unknown mechanism. Therefore, it is important to explore the underlying mechanism of CPSP. In the present study, a CPSP model was induced by thalamic hemorrhage using Coll IV injection with using the research method from a previous study as reference (27). The results demonstrated that thalamic hemorrhagic stroke, resulting from microinjection of Coll IV into the VPL nucleus, led to pain hypersensitivities, such as thermal hyperalgesia, mechanical allodynia and cold allodynia in a mouse model, which may imitate thalamic pain arising from hemorrhagic stroke in the clinic. Comprehension of the underlying mechanism of hemorrhage-induced thalamic pain allows for the development of innovative therapeutic strategies for preventing and treating the disease. The present study also indicated that astrocyte activation (detected via GFAP) may occur in the Coll IV-induced CPSP model. The results demonstrated that miR-223 and the NLRP3 inflammasome participated in the development of thalamic hemorrhagic stroke-induced pain. miR-223 expression levels were significantly decreased in the CPSP model, and injection of a miR-223 agomir significantly attenuated thalamic pain (including mechanical, thermal and cold sensitivity) and significantly lowered proinflammatory cytokine (IL-18 and IL-1β) protein expression levels. However, microinjection with the miR-223 antagomir into the VPL nucleus of naïve mice mimicked thalamic pain and significantly increased proinflammatory cytokine (IL-18 and IL-1β) protein expression levels. The present study also indicated that miR-223 may ease CPSP by targeting the NLRP3 inflammasome signaling cascade.

Previous studies have reported that miRNAs have a vital function in neuropathic pain (40-42). For example, miR-195 upregulation occurs in spinal microglia of rats with spinal nerve ligation and exacerbates neuropathic pain by impeding autophagy following peripheral nerve injury (43). However, the role of miRNAs in CPSP are still unknown. miR-223 has

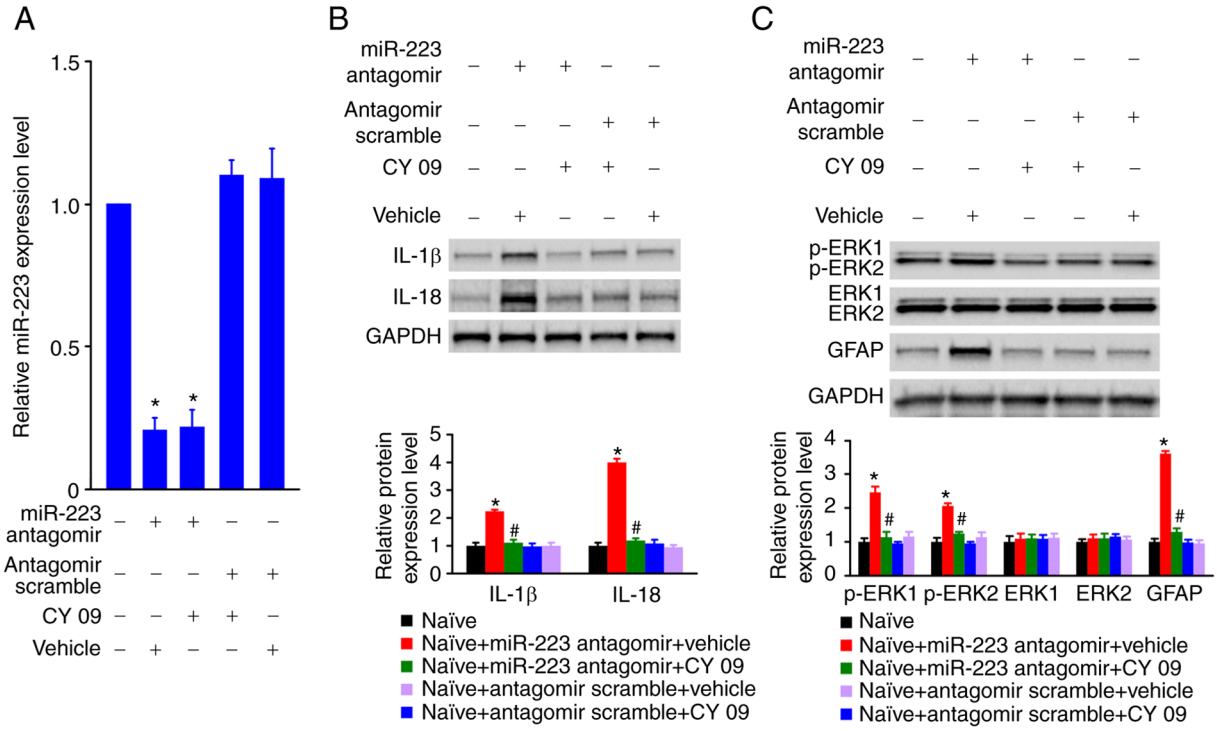

Figure 8. CY 09 affects IL-18, IL-1β, p-ERK1/2 and GFAP protein expression levels. (A) CY 09 injection caused no alterations in miR-223 expression levels. CY 09 injection (B) significantly reduced IL-18 and IL-1β protein expression levels in the naïve + miR-223 antagomir cohort and (C) significantly lowered the protein expression levels of GFAP and p-ERK1/2. n=3 mice/cohort. *P<0.05 vs. naïve group; #P<0.05 vs. miR-223 antagomir + vehicle. GFAP, glial fibrillary acidic protein; p, phosphorylated; miR, microRNA.

been extensively examined and been found to contribute to vital functions in numerous diseases, including cancer (44,45) and inflammatory diseases (46). Moreover, miR-223 has a critical function in the nervous system. Cressatti *et al* (47) demonstrated that the salivary miR-223 level is considerably reduced in patients with Parkinson's disease. However, the association between miR-223 and CPSP remains to be elucidated. In the present study, it was demonstrated that miR-223 has a suppressive function by targeting NLRP3 in mice with CPSP. The results determined that miR-223 expression levels were significantly reduced following thalamic hemorrhage, overexpression of miR-223 significantly ameliorated CPSP and inhibition of miR-223 in naïve mice mimicked CPSP. These results indicated that the downregulation of miR-223 after thalamic hemorrhage may contribute to CPSP development. These findings indicated that miR-223 may inhibit CPSP by inhibiting NLRP3-triggered neuroinflammation, therefore offering fresh insight into the molecular pathogenesis of CPSP.

Among all NLR inflammasomes, NLRP3 is the most comprehensively understood because it has been widely studied in respect to certain diseases, such as inherited autoinflammatory syndromes (48) and certain metabolic diseases (49). Recently, NLRP3 inflammasome function has been studied in the CNS and the NLRP3 inflammasome has been found to contribute to crucial functions in the development of bacterial meningitis and Alzheimer's disease (50). In the present study, the NLRP3 inflammasome proteins ASC and NLRP3, as well as the downstream factors caspase-1, IL-18 and IL-1β, were significantly elevated in the thalamus of CPSP mice. Furthermore, the results demonstrated that by blocking NLRP3 inflammasome activity or expression pain hypersensitivities, such as cold allodynia, mechanical allodynia and thermal hyperalgesia, were significantly attenuated. These findings indicated that CPSP may induce NLRP3 inflammasome activation and subsequent cleavage of IL-18 and IL-1β. Thalamus injection of miR-223 agomir 3 days before Coll IV injection significantly ameliorated thalamus hemorrhage-induced CPSP, such as cold allodynia, mechanical allodynia and thermal hyperalgesia. The analgesic effects of overexpressed miR-223 were potentially associated with a significant reduction in caspase-1, ASC, NLRP3, IL-18 and IL-1β protein expression levels. Furthermore, the results of the dual-luciferase reporter assay indicated that miR-223 may target the 3'UTR of NLRP3 mRNA to inhibit NLRP3 expression. The rescue experiment performed in the present study demonstrated that mimicking CPSP via miR-223 inhibition in naïve mice was significantly reversed by administration of an NLRP3 inhibitor. These results indicated that miR-223 downregulation may result in CPSP via the upregulation of NLRP3. Further, it was also demonstrated that CPSP induced the activation of astrocytes and neuronal damage. Microinjection of the miR-223 agomir into the thalamus significantly reversed this result, likely due to mediation of the role of the miR-223 agomir by neurons and the activation of astrocytes by injured neurons. Together, these results suggested that miR-223 and NLRP3 inflammasomes may participate in the pathogenesis of CPSP.

IL-1β is produced as an antecedent, pro-IL-1β, which then must be cleaved by caspase-1 to become biologically active (51). The present study demonstrated that the NLRP3 inflammasome, the best-characterized inflammasome activated by cellular stress or infection, led to CPSP development

via induction of IL-1β cleavage. miR-223 overexpression significantly inhibited this signaling pathway and may therefore serve as an efficacious analgesic in pain management.

In summary, the experimental data in the present study demonstrated that miR-223 inhibited the activity of the NLRP3 inflammasome (caspase-1, ASC and NLRP3), which ameliorated thalamus hemorrhage-induced CPSP in mice via the downregulation of NLRP3. However, the mechanisms of NLRP3 and miR-223 in CPSP occurrence, development and prognosis require further validation because miR-223 expression at the cellular level was not ascertained in the present study.

Acknowledgements

Not applicable.

Funding

The present study was supported by The National Natural Science Foundation of China (grant nos. 81571936 and 81601679).

Availability of data and materials

The datasets used and/or analyzed during the current study are available from the corresponding author on reasonable request.

Authors' contributions

JG conceived the project and supervised all experiments. TH, CW, YZ and JG designed the project. XC and YL performed the molecular and biochemical experiments. YX constructed the animal models, performed behavioral tests and revised the manuscript. YG analyzed the data. TH wrote the manuscript draft. JG edited the manuscript. TH and YX confirm the authenticity of all the raw data. All authors have read, discussed and approved the final manuscript.

Ethics approval and consent to participate

The research protocol and animal experiments were approved by the Animal Care and Use Committee of the Medical College of Yangzhou University (Yangzhou, China; approval no. SYXK2017-0044).

Patient consent for publication

Not applicable.

Competing interests

The authors declare that they have no competing interests.

References

1. Maida CD, Norrito RL, Daidone M, Tuttolomondo A and Pinto A: Neuroinflammatory mechanisms in ischemic stroke: Focus on cardioembolic stroke, background, and therapeutic approaches. Int J Mol Sci 21: 6454, 2020.
2. Paolucci S, Iosa M, Toni D, Barbanti P, Bovi P, Cavallini A, Candeloro E, Mancini A, Mancuso M, Monaco S, *et al*: Prevalence and time course of post-stroke pain: A multicenter prospective hospital-based study. Pain Med 17: 924-930, 2016.
3. Harrison RA and Field TS: Post stroke pain: Identification, assessment, and therapy. Cerebrovasc Dis 39: 190-201, 2015.
4. Klit H, Finnerup NB and Jensen TS: Central post-stroke pain: Clinical characteristics, pathophysiology, and management. Lancet Neurol 8: 857-868, 2009.
5. Vukojevic Z, Dominovic Kovacevic A, Peric S, Grgic S, Bjelica B, Basta I and Lavrnic D: Frequency and features of the central poststroke pain. J Neurol Sci 391: 100-103, 2018.
6. Feigin VL, Lawes CM, Bennett DA and Anderson CS: Stroke epidemiology: A review of population-based studies of incidence, prevalence, and case-fatality in the late 20th century. Lancet Neurol 2: 43-53, 2003.
7. Kumar G and Soni CR: Central post-stroke pain: Current evidence. J Neurol Sci 284: 10-17, 2009.
8. Kumar B, Kalita J, Kumar G and Misra UK: Central poststroke pain: A review of pathophysiology and treatment. Anesth Analg 108: 1645-1657, 2009.
9. Martinon F, Burns K and Tschopp J: The inflammasome: A molecular platform triggering activation of inflammatory caspases and processing of proIL-beta. Mol Cell 10: 417-426, 2002.
10. Huang Y, Xu W and Zhou R: NLRP3 inflammasome activation and cell death. Cell Mol Immunol 18: 2114-2127, 2021.
11. Leemans JC, Cassel SL and Sutterwala FS: Sensing damage by the NLRP3 inflammasome. Immunol Rev 243: 152-162, 2011.
12. Li WW, Guo TZ, Liang D, Shi X, Wei T, Kingery WS and Clark DJ: The NALP1 inflammasome controls cytokine production and nociception in a rat fracture model of complex regional pain syndrome. Pain 147: 277-286, 2009.
13. Chen L, Li X, Huang L, Wu Q, Chen L and Wan Q: Chemical stimulation of the intracranial dura activates NALP3 inflammasome in trigeminal ganglia neurons. Brain Res 1566: 1-11, 2014.
14. Smith HS, Bracken D and Smith JM: Gout: Current insights and future perspectives. J Pain 12: 1113-1129, 2011.
15. Zhang A, Wang K, Ding L, Bao X, Wang X, Qiu X and Liu J: Bay11-7082 attenuates neuropathic pain via inhibition of nuclear factor-kappa B and nucleotide-binding domain-like receptor protein 3 inflammasome activation in dorsal root ganglions in a rat model of lumbar disc herniation. J Pain Res 10: 375-382, 2017.
16. Qian J, Zhu W, Lu M, Ni B and Yang J: D-β-hydroxybutyrate promotes functional recovery and relieves pain hypersensitivity in mice with spinal cord injury. Br J Pharmacol 174: 1961-1971, 2017.
17. Liu J: Control of protein synthesis and mRNA degradation by microRNAs. Curr Opin Cell Biol 20: 214-221, 2008.
18. Sakai A, Saitow F, Miyake N, Miyake K, Shimada T and Suzuki H: miR-7a alleviates the maintenance of neuropathic pain through regulation of neuronal excitability. Brain 136: 2738-2750, 2013.
19. Leinders M, Üçeyler N, Pritchard RA, Sommer C and Sorkin LS: Increased miR-132-3p expression is associated with chronic neuropathic pain. Exp Neurol 283: 276-286, 2016.
20. Gilicze AB, Wiener Z, Tóth S, Buzás E, Pállinger É, Falcone FH and Falus A: Myeloid-derived microRNAs, miR-223, miR27a, and miR-652, are dominant players in myeloid regulation. BioMed Res Int 2014: 870267, 2014.
21. Wang J, Bai X, Song Q, Fan F, Hu Z, Cheng G and Zhang Y: miR-223 inhibits lipid deposition and inflammation by suppressing toll-like receptor 4 signaling in macrophages. Int J Mol Sci 16: 24965-24982, 2015.
22. Cardoso AL, Guedes JR and de Lima MC: Role of microRNAs in the regulation of innate immune cells under neuroinflammatory conditions. Curr Opin Pharmacol 26: 1-9, 2016.
23. Bauernfeind F, Rieger A, Schildberg FA, Knolle PA, Schmid-Burgk JL and Hornung V: NLRP3 inflammasome activity is negatively controlled by miR-223. J Immunol 189: 4175-4181, 2012.
24. Haneklaus M, Gerlic M, Kurowska-Stolarska M, Rainey AA, Pich D, McInnes IB, Hammerschmidt W, O'Neill LA and Masters SL: Cutting edge: miR-223 and EBV miR-BART15 regulate the NLRP3 inflammasome and il-1β production. J Immunol 189: 3795-3795-3799, 2012.
25. General Administration of Quality Supervision, Inspection and Quarantine of the People's Republic of China, Standardization Administration of China. Laboratory animal - Requirements of environment and housing facilities GB 14925-2010[S]. China Quality Inspection Press, Beijing, pp1-18, 2010.
26. Zimmermann M: Ethical guidelines for investigations of experimental pain in conscious animals. Pain 16: 109-110, 1983.

27. Cai W, Wu S, Pan Z, Xiao J, Li F, Cao J, Zang W and Tao YX: Disrupting interaction of PSD-95 with nNOS attenuates hemorrhage-induced thalamic pain. Neuropharmacology 141: 238-248, 2018.
28. Li Z, Mao Y, Liang L, Wu S, Yuan J, Mo K, Cai W, Mao Q, Cao J, Bekker A, *et al*: The transcription factor C/EBPβ in the dorsal root ganglion contributes to peripheral nerve trauma-induced nociceptive hypersensitivity. Sci Signal 10: eaam5345, 2017.
29. Li Z, Gu X, Sun L, Wu S, Liang L, Cao J, Lutz BM, Bekker A, Zhang W and Tao YX: Dorsal root ganglion myeloid zinc finger protein 1 contributes to neuropathic pain after peripheral nerve trauma. Pain 156: 711-721, 2015.
30. Xu JT, Zhao JY, Zhao X, Ligons D, Tiwari V, Atianjoh FE, Lee CY, Liang L, Zang W, Njoku D, *et al*: Opioid receptor-triggered spinal mTORC1 activation contributes to morphine tolerance and hyperalgesia. J Clin Investig 124: 592-603, 2014.
31. Zhao X, Tang Z, Zhang H, Atianjoh FE, Zhao JY, Liang L, Wang W, Guan X, Kao SC, Tiwari V, *et al*: A long noncoding RNA contributes to neuropathic pain by silencing Kcna2 in primary afferent neurons. Nat Neurosci 16: 1024-1031, 2013.
32. Huang T, Fu G, Gao J, Zhang Y, Cai W, Wu S, Jia S, Xia S, Bachmann T, Bekker A and Tao YX:Fgr contributes to hemorrhage-induced thalamic pain by activating NF-κB/ERK1/2 pathways. JCI Insight 5:e139987, 2020.
33. Fang XZ, Huang TF, Wang CJ, Ge YL, Lin SY, Zhang Y and Gao J: Preconditioning of physiological cyclic stretch attenuated HMGB1 expression in pathologically mechanical stretch-activated A549 cells and ventilator-induced lung injury rats through inhibition of IL-6/STAT3/SOCS3. Int Immunopharmacol 31: 66-73, 2016.
34. Zhang Y, Huang T, Jiang L, Gao J, Yu D, Ge Y and Lin S: MCP-induced protein 1 attenuates sepsis-induced acute lung injury by modulating macrophage polarization via the JNK/c-Myc pathway. Int Immunopharmacol 75: 105741, 2019.
35. Livak KJ and Schmittgen TD: Analysis of relative gene expression data using real-time quantitative PCR and the 2-(-Delta Delta C(T)) method. Methods 25: 402-408, 2001.
36. Yu D, Fang X, Xu Y, Xiao H, Huang T, Zhang Y, Ge Y, Li Y, Zong L and Gao J: Rev-erbα can regulate the NF-κB/NALP3 pathway to modulate lipopolysaccharide-induced acute lung injury and inflammation. Int Immunopharmacol 73: 312-320, 2019.
37. Jiang H, He H, Chen Y, Huang W, Cheng J, Ye J, Wang A, Tao J, Wang C, Liu Q, *et al*: Identification of a selective and direct NLRP3 inhibitor to treat inflammatory disorders. J Exp Med 214: 3219-3238, 2017.
38. Yang Y, Yang F, Yang F, Li CL, Wang Y, Li Z, Lu YF, Yu YQ, Fu H, He T, *et al*: Gabapentinoid Insensitivity after Repeated Administration is Associated with Down-Regulation of the α(2) δ-1 Subunit in rats with central post-stroke pain hypersensitivity. Neurosci Bull 32: 41-50, 2016.
39. Wang J: Preclinical and clinical research on inflammation after intracerebral hemorrhage. Prog Neurobiol 92: 463-477, 2010.
40. Pan Z, Shan Q, Gu P, Wang XM, Tai LW, Sun M, Luo X, Sun L and Cheung CW: miRNA-23a/CXCR4 regulates neuropathic pain via directly targeting TXNIP/NLRP3 inflammasome axis. J Neuroinflammation 15: 29, 2018.
41. Wang Z, Liu F, Wei M, Qiu Y, Ma C, Shen L and Huang Y: Chronic constriction injury-induced microRNA-146a-5p alleviates neuropathic pain through suppression of IRAK1/TRAF6 signaling pathway. J Neuroinflammation 15: 179, 2018.
42. Shi J, Jiang K and Li Z: miR-145 ameliorates neuropathic pain via inhibiting inflammatory responses and mTOR signaling pathway by targeting Akt3 in a rat model. Neurosci Res 134: 10-17, 2018.
43. Shi G, Shi J, Liu K, Liu N, Wang Y, Fu Z, Ding J, Jia L and Yuan W: Increased miR-195 aggravates neuropathic pain by inhibiting autophagy following peripheral nerve injury. Glia 61: 504-512, 2013.
44. Correction to title, results, and conclusion in: Down-regulated IncRNA F630028O10Rik contributes to suppress lung cancer in mice through inhibiting miR-223-3p and VEGF signaling pathway. Chest 150: 261, 2016.
45. Yang F, Xu Y, Liu C, Ma C, Zou S, Xu X, Jia J and Liu Z: NF-κB/miR-223-3p/ARID1A axis is involved in Helicobacter pylori CagA-induced gastric carcinogenesis and progression. Cell Death Dis 9: 12, 2018.
46. Calvente CJ, Tameda M, Johnson CD, del Pilar H, Lin YC, Adronikou N, De Mollerat Du Jeu X, Llorente C, Boyer J and Feldstein AE: Neutrophils contribute to spontaneous resolution of liver inflammation and fibrosis via microRNA-223. J Clin Investig 129: 4091-4109, 2019.
47. Cressatti M, Juwara L, Galindez JM, Velly AM, Nkurunziza ES, Marier S, Canie O, Gornistky M and Schipper HM: Salivary microR-153 and microR-223 levels as potential diagnostic biomarkers of idiopathic Parkinson's disease. Mov Disord 35: 468-477, 2019.
48. Hoffman HM, Mueller JL, Broide DH, Wanderer AA and Kolodner RD: Mutation of a new gene encoding a putative pyrin-like protein causes familial cold autoinflammatory syndrome and Muckle-Wells syndrome. Nat Genet 29: 301-305, 2001.
49. Wen H, Ting JP and O'Neill LA: A role for the NLRP3 inflammasome in metabolic diseases-did Warburg miss inflammation? Nat Immunol 13: 352-357, 2012.
50. Liu SB, Mi WL and Wang YQ: Research progress on the NLRP3 inflammasome and its role in the central nervous system. Neurosci Bull 29: 779-787, 2013.
51. Guo S, Yang C, Diao B, Huang X, Jin M, Chen L, Yan W, Ning Q, Zheng L, Wu Y and Chen Y: The NLRP3 inflammasome and IL-1β accelerate immunologically mediated pathology in experimental viral fulminant hepatitis. PLoS Pathog 11: e1005155, 2015.